

1 **Rockslides on limestone cliffs with sub-horizontal bedding in the southwestern calcareous**  
2 **area, China**

3

4 Authors: Z. Feng<sup>1</sup>, Y.P. Yin<sup>2</sup>, B. Li<sup>1</sup>, K. He<sup>3</sup>

5 1. Key Laboratory of Neotectonic Movement and Geohazard of MLR at Institute of

6 Geomechanics, Chinese Academy of Geological Science, Beijing 100081, China.

7 2. China Institute of Geo-Environment Monitoring, Beijing 100081, China

8 3. Chang'an University, Xi'an 710054, China

9 \*. Correspondence to: B. Li. (libin1102@163.com, +86-010-88815022)

10

11 **Abstract:** Calcareous mountainous areas are highly prone to geohazards, and rockslides play an  
12 important role in cliff retreat. This study presents three examples of failures of limestone cliffs  
13 with sub-horizontal bedding in the southwestern calcareous area of China. Field observations and  
14 numerical modeling of Yudong Escarpment, Zengzi Cliff, and Wangxia Cliff showed that  
15 pre-existing vertical joints passing through thick limestone and the alternation of competent and  
16 incompetent layers are the most significant features for rockslides. A “hard on soft” cliff made of  
17 hard rocks superimposed of soft rocks is prone to rock slump, characterized by shearing through  
18 the underlying weak strata along a curved surface and backward tilting. When a slope contains  
19 weak interlayers rather than a soft basal, a rock collapse could occur from the compression  
20 fracture and tensile split of the rock mass near the interfaces. A rock slide might shear through a  
21 hard rock mass if no discontinuities are exposed in the cliff slope, and sliding may occur along a  
22 moderately inclined rupture plane. The “toe breakout” mechanism mainly depends on the strength

批注 [11]: The “layers” is deleted

23 characteristics of the rock mass.

24 **Key words:** cliff failure; sub-horizontal bedding; plane slide; toe splitting; rock slump; numerical  
25 modeling

26

## 27 **1. Introduction**

28 The southwestern calcareous area of China covers a large area of  $54.4 \times 10^3 \text{ km}^2$ , and it is highly  
29 prone to geohazards. Many multilayered carbonate rocks with sub-horizontal bedding have been  
30 deeply cut by rivers during crustal uplift and form significant topographic relief in steep slopes  
31 and cliffs. These sub-horizontal cliff slopes are usually dominated by two sets of sub-vertical  
32 conjugate joints and are characterized by slightly folded or faulted to massive rock masses.  
33 Rockslides from sub-horizontally bedded cliff failure and resulting catastrophes have occurred  
34 widely and frequently in the southwestern calcareous area of China.

35 Considerable research on cliff failure has been conducted in similar areas around the world(Abele,  
36 1994; Von, 2002; Rohn, 2004; Embleton, 2007; Ruff, et al., 2008; Palma, et al., 2012), such as the  
37 North Calcareous Alps in Austria. It is believed that water, lithology, geological structure, and  
38 karstification are of primary importance in triggering rockslides from cliff failure (Kay, et al.,  
39 2006). These factors dominate the tearing and shearing failure mechanism of the rock masses and  
40 joints, which are directly displayed in the consequent failure behavior of the cliff slopes. Types of  
41 rockslides with different detachment mechanisms (slumps, plane slides, topples, and lateral  
42 spreading) in sub-horizontally bedded cliffs with particular geological settings and triggering  
43 mechanisms have been described by engineering geologists, e.g., the collapse of the Mt. Sandling  
44 and Mt. Raschberg limestone towers had a complex failure sequence from lateral spread to

45 toppling followed by rock fall (Rohn, et al., 2004). In addition to lateral spreading, a cliff slope  
46 with a geological formation of hard rock on a soft base may undergo the translational sliding or  
47 slumping of slab-shaped blocks (Poisel, 2005). In addition, the karst process is an inevitable factor  
48 in rockslide formation. Tectonic joints keep widening and extending to the deep of rock mass by  
49 constant dissolution and disgregation of underground water, forming boundaries of perilous rocks  
50 (Santo, et al., 2007). It is believe that karst plays an important role in rockslides from carbonate  
51 mountains, especially for gently bedding-inclined slopes which are unfavorable to failure.

52 Active underground mining is widespread in the southwestern calcareous area of China. There is  
53 the potential for damage to cliff faces and overhangs when mining activity occurs beneath cliffs.  
54 This has been repeatedly shown to be true. Taking the Southern Coalfields of Australia as an  
55 example, several types of cliff failure have been witnessed in the goaf area, although no  
56 instabilities have been reported beyond the mining area (Kay, 2006). However, there is no  
57 available and widely accepted model that can predict the failure susceptibility of steep slopes close  
58 to mining. This is because of the complex interaction of factors influencing the stability of steep  
59 slopes, which include geometry, geology, geological structure, environmental factors, and  
60 technical mining parameters. An integrated method combining landslide science and mining  
61 subsidence science is promising as a direction for future research.

62 This study focuses on the failure mechanisms of cliffs with sub-horizontal bedding in the  
63 southwestern calcareous area of China and the recognition of these features in field investigations.  
64 The three cases presented occurred during the last 10 years and caused great damage to both  
65 human life and assets. Furthermore, post-failure behavior, such as rock avalanches and debris  
66 flows, is not included in descriptions of failure mechanisms of steep slopes. The term “failure

67 mechanism” in this study particularly refers to the detachment mechanism of rock masses from the  
68 cliff slope.

69

## 70 2. Geological background

71 According to the Geo-hazards Survey Plan lunched by Ministry of Land and Resources of China  
72 since 1999, most of the counties and cities in the southwestern calcareous China are most serious  
73 area suffering from geo-hazards (Zhang et al, 2000; Li et al, 2004). The likelihood of rockslide  
74 instability in the area is high, mainly because of the local geological evolution. Tectonic  
75 movement during the Mesozoic was characterized by compression and formed the area into a fold  
76 belt, mainly striking NNE (Fig.1). Neotectonic uplift raised the thick carbonate rocks to high  
77 altitude and shaped the steep and folded landforms.

**批注 [S2]:** Q: The influence of karst and softer layer were discussed well, but the title of this section is geological background, so I suggest that add a column lithology map about the detailed P & T time, including the hard rock and soft interbed. The reviewer will make it clear that why the soft and karst are very important.  
A: A rock sequence is added and listed in Figure 2. Orders of the figures is revised. And the lithology is also described in line 76-90 and are introduced respectively in each case. In addition, stratigraphic profiles in section 3 showed the interbedded limestone and weak shale.

**批注 [I3]:** Q: more detailed information about the region is need.  
A: Line 71-73 and relative references are added as proof of geo-hazards highly prone area.

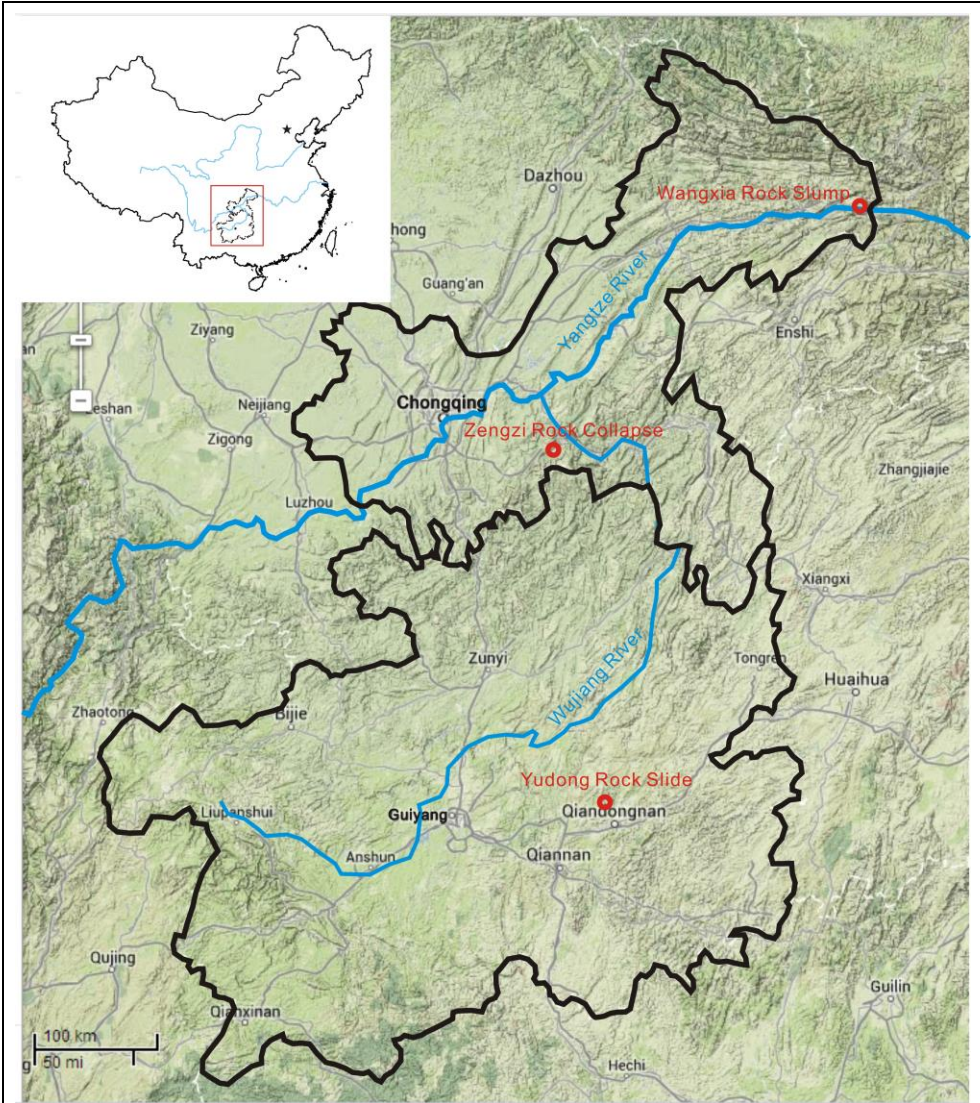


Fig. 1 Locations of three rockslides: Wangxia Rock Slump, Zengzi Rock Collapse, and Yudong Rock Slide.

批注 [14]: Q: If you can add the lithology or the strata into the map, it is better. Meanwhile, the region should be introduced in the 2 section.  
 A: Figure 1 is moved from section 3 to section 2. Figure 1 meant to show the regional terrain (line 74-77) and location of three cases. The lithology column is inserted in section 2 and the stratigraphic profiles in section 3 also show the strata.

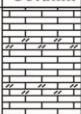
System	Series	Symb	Column	Thickness	Lithology
Triassic	Lower	$T_1^2$		520~650m	layered limestone and dolomite, usually in cliff landform.
		$T_1^1$		660~680m	mudstone, layered limestone, dolomitic limestone, locally contains shale bands.
Permian	Upper	$P_3^2$		95~134m	layered limestone, usually be shaped into cliffs.
		$P_3^1$		98~143m	layered to blocky limestone rock, underlain by a measure of claystone, shale, and coal seams
	Middle	$P_2^3$		203~377m	layered to blocky limestone rock, interbedded with carbonaceous shale, usually cut by conjugate joints and in cliff landform.
		$P_2^2$		47~106m	thick layered limestone, interbedded with argillaceous bands, usually cut by joints and in cliff landform.
		$P_2^1$		2~13m	claystone, carbonaceous shale, interbedded with coal seams, bauxite, shaped into steep slope under the hard cap rocks
Silurian	Middle	$S_2$		500~680m	shale, silty shale, easily weathered and usually in a landform of gentle slopes

Fig.2 The most common outcrop sequence in southwest calcareous China

78

79 Many layers of carbonate rocks were deposited from Permian until Triassic time, and were  
80 interbedded with weak planes or soft strata (Fig.2). The carbonate rock masses possess great  
81 strength and integrity; thus, they usually form steep slopes hundreds of meters high, e.g., the Three  
82 Gorges, if there are no intercalated soft strata. Under these circumstances, slope movement is  
83 mainly controlled by discontinuities such as weak interlayers, karst, and fissures. The thick  
84 carbonate succession in the southwestern calcareous area of China contains multiple layers of  
85 weak shale planes, including carbonaceous shale and pyrobituminous shale. The strength of the  
86 shale planes is relatively low and significantly varies with the weathering process, from virgin  
87 rock to fractured planes to argillaceous layers. The strength of carbonaceous shale sandwiched in  
88 the  $P_1$  limestone at Lianziya Cliff is low that the cohesion and internal friction angle are 0.08–0.39  
89 MPa,  $18^\circ$ – $21^\circ$  and 0.06–0.078 MPa,  $18^\circ$ – $19.8^\circ$  for dry and saturated samples, respectively (Ding,

批注 [15]: The “argillated” is replaced by “argillaceous”

批注 [16]: Q: The geological age should be marked consistently only using symbols or texts.

A: The texts are replaced by symbols.

90 et al. 1990). The weak interlayers play a significant role in mass movement. When soft strata  
91 underlie hard rock, the yielding of the soft base may cause the uneven subsidence of the cap rock.  
92 Lateral spreading and slumps with backward tilting are caused by this type of destabilization  
93 mechanism, in which failure propagates uphill.

94 In the southwestern calcareous area of China, coal measures are common soft strata, accompanied  
95 by thick carbonate sequences. Except for coal seams, the coal measures are usually composed of  
96 associated interlayers of shale, carbonaceous shale, pyrobituminous shale, and bauxitic claystone.  
97 Mining is active in these coal measures using the techniques of room and pillar mining and  
98 longwall mining. The depth of cover ranges from dozens to hundreds of meters. It is believed that  
99 underground mining activities can change the engineering geological conditions and reduce the  
100 stability of cliffs (Tang, 2009; Altun, et al., 2010; Marschalko, et al., 2012; Lollino, et al., 2013), .  
101 Cliff failures and the resulting catastrophes, examples of which are discussed below, are related to  
102 underground mining.

103 Karstification is a significant factor when discussing the reasons for carbonate slope failure. It  
104 particularly affects steeply inclined faults and tectonic joints and slowly widens the discontinuities  
105 to create large open fractures, which foster rockslides (Santo et al., 2007; Parise, 2008). In  
106 addition, the karstification process can cause a significant reduction in the mechanical properties  
107 of the carbonate rock mass. This is very important for toe-constrained slides, which depend on the  
108 strength of the rock mass at the toe. In some cases, the underground karst voids play the same role  
109 as goaf, and cavern breakdown may also lead to landslides (White, et al., 1969; Parise, 2010).

110

111 **3. Failure modes**

112 Different types of rockslides have been observed in thickly and sub-horizontally bedded limestone  
113 escarpments. Gently inclined bedding is unfavorable for large translational slides. Slope failures,  
114 including slide, collapse and slump, are discussed below in detail to explain their mechanisms.

115 Three examples are given: the Yudong Escarpment, Zengzi Cliff, and Wangxia Cliff (Fig. 1).

116 **3.1 Rock slide at the Yudong Escarpment**

117 On February 18, 2013, a rock slide occurred in Longchang County, Guizhou Province. The  
118 mass movement is located in a high and steep bank of the Yudong River, close to an underground  
119 mining area (Fig. 3). The S308 provincial road runs on the opposite bank of the river. The rock  
120 slide buried several houses and five people beneath the escarpment and blocked the river.

批注 [17]: Q: "Failure modes" is more accurate  
A: Suggestion is taken.

批注 [18]: Q: inaccurate expressions  
A: The sentence is rewritten as in the text.

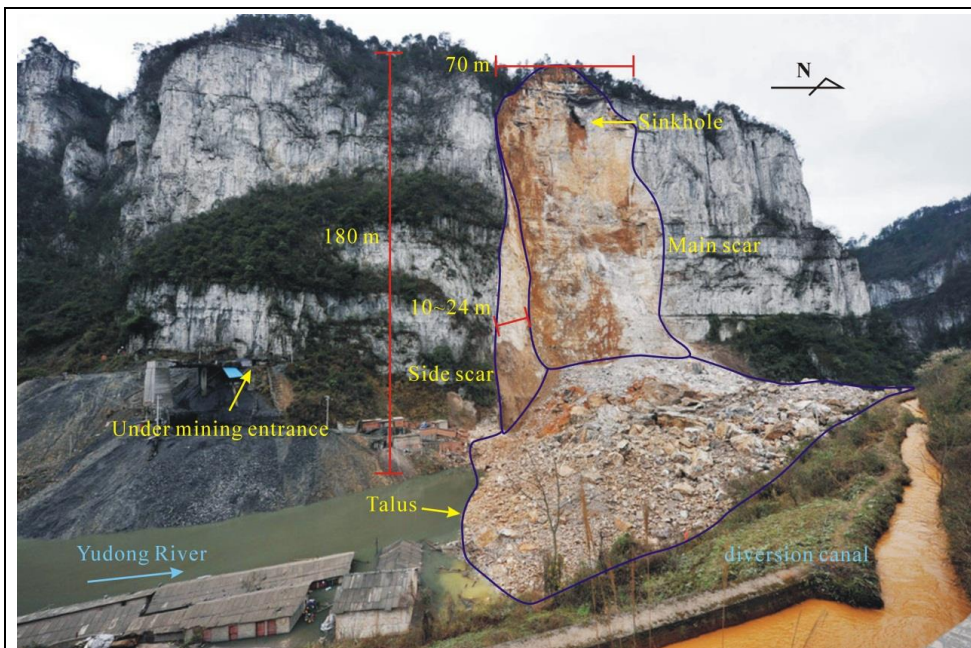


Fig. 3 Photograph showing an overview of Yudong rock slide I.

121

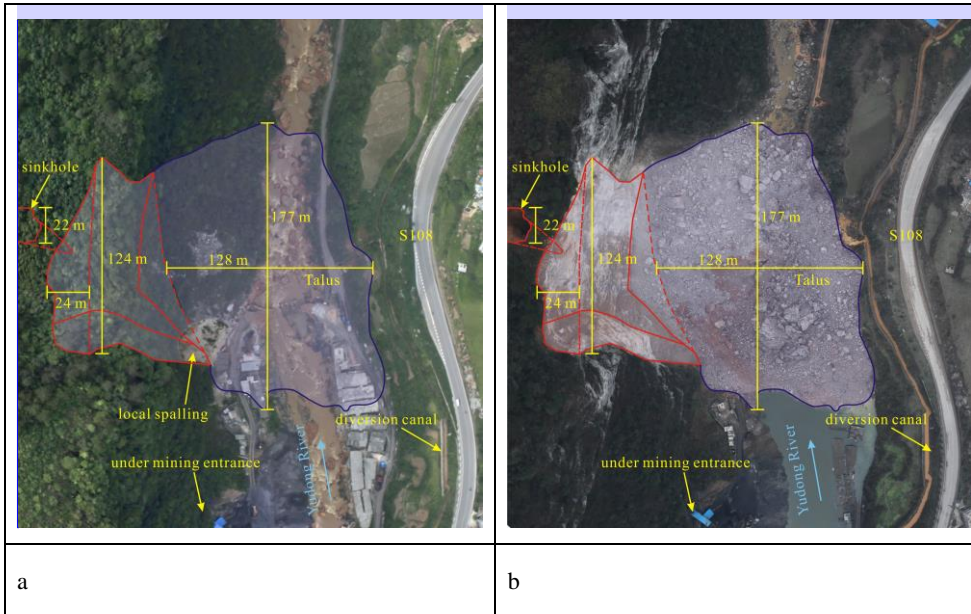
122 The Yudong Escarpment is about 220 m high and the slope angle is more than 80°. The steep

123 slope faces in the direction SE100°-130°, and the dip direction is NW325°, with slightly inclined  
124 bedding. The outcrop consists of thickly bedded  $P_2^2$  limestone and underlying  $P_2^1$  coal measures.  
125 The Yudong Escarpment lies in the gentle eastern flank of the Yudong Syncline, which strikes  
126 NNE. As a result, a set of NNE-trending joints and a conjugate set of NW-trending joints are  
127 present in the rock mass. The orthogonal 130°/70° and 80°/75° joints cut the 325°/9° rock  
128 beds into prism- and tower-shaped blocks on the edge of the cliff. The jointed limestone is  
129 moderately weathered, and the uniaxial compression strength of intact rock reaches 30 MPa. The  
130 coal measures are composed of thickly bedded argillaceous shale and coal seams. Coal extraction  
131 has been active in the soft basal unit, and the goaf is about 200 m deep behind the cliff face. The  
132 “2.18” Yudong rock slide originates from one of these unstable blocks with a volume of about 30  
133  $\times 10^4$  m<sup>3</sup>. Several types of karst are observed in the rock slide area, including sinkholes, karst  
134 tunnels, and dissolution fissures. A remote sensing image taken the day after the rock collapse  
135 shows a sinkhole at the crest with a diameter of 2.2 m immediately behind the fall. The pipe flow  
136 in the tunnels and cracks induce static and dynamic pressure, acting on the unstable rock block  
137 and changing the stability. However, because of abundant vegetation, the sinkhole is not visible in  
138 a previous image that was taken in the summer of 2012 (Fig. 4). The intense karstic erosion of a  
139 yellowish-orange color has been observed on the vertical scar. The selective karst widens and  
140 connects the pre-existing steep joints so that the area of the rock bridge covers less than 30% of  
141 the main scar (Huang, 2013). The directed scratches indicate the brittle failure of the rock bridges  
142 and consequent fall of the rock mass. The rock slide left two scars originate from joints. The main  
143 scar is nearly parallel to the cliff face and about 80 m wide. The upper part of the main scar is a  
144 sub-vertical plane, and the lower parts are planar and dip out of the cliff. The conjugate side scar is

**批注 [19]:** Q:I suggest that this highlight sentences move behind the explanation of its tectonic and its structural planes.  
A: The sentence is moved behind as suggested.

**批注 [110]:** Q: I am not sure what it means.  
A: It is rewritten as in the text.

145 about 24 m wide and perpendicular to the cliff face (Fig.3).



批注 [S11]: The two pictures are switched in order.

Fig.4 Aerial photos of Rock Slide Itaken in summer 2012 (a) and on February 19 2013 (b). The zoning of the depleted mass and talus is projected in picture (a) prior to the catastrophe. The abundant vegetation and steep terrain make it difficult to distinguish the potential failure. However, there were signs of local spalling at the toe of the cliff face (a). A 22-m-diameter sinkhole was exposed in winter, which connected with the main back scar of the rock slide (b).

146

147 Another massive rock slide (II) (Fig. 5) occurred on April 16, 2013, about 100 m away from the  
148 February 18 rock slide (I). The morphology of the vertical scar of rock slide II is similar to that of  
149 rock slide I. The lower rupture surface forms a steep and irregular scar (Fig. 6). These two rock  
150 slides have the same failure mechanism of a steep back scar separating the unstable block from the  
151 escarpment and the block breaking through the toe leading to free fall of the rock mass. The  
152 rupture surface implies a plane slide involving shear failure through the rock mass. There is little  
153 or no shear displacement along the rupture surface, and the velocity is very high. The brittle

154 failure of the rock mass in the toe area can be explained by the brittle failure of the rock mass  
155 under uniaxial compression tests. In other words, it is largely dependent on the mechanical  
156 properties of the rock mass at the toe. The toe is sheared along random discontinuities of limited  
157 persistence traced by the rupture surface (Fig. 7).



批注 [S12]: The old picture is replaced by a new one with borders.

Fig. 5 Rock slide II is located north of rock slide I and has the same geological conditions, except for undermining. The volume of the talus of rock slide II is  $30 \times 10^4 \text{ m}^3$ . It blocked the Yudong River and covered 80 m of the S308 road.

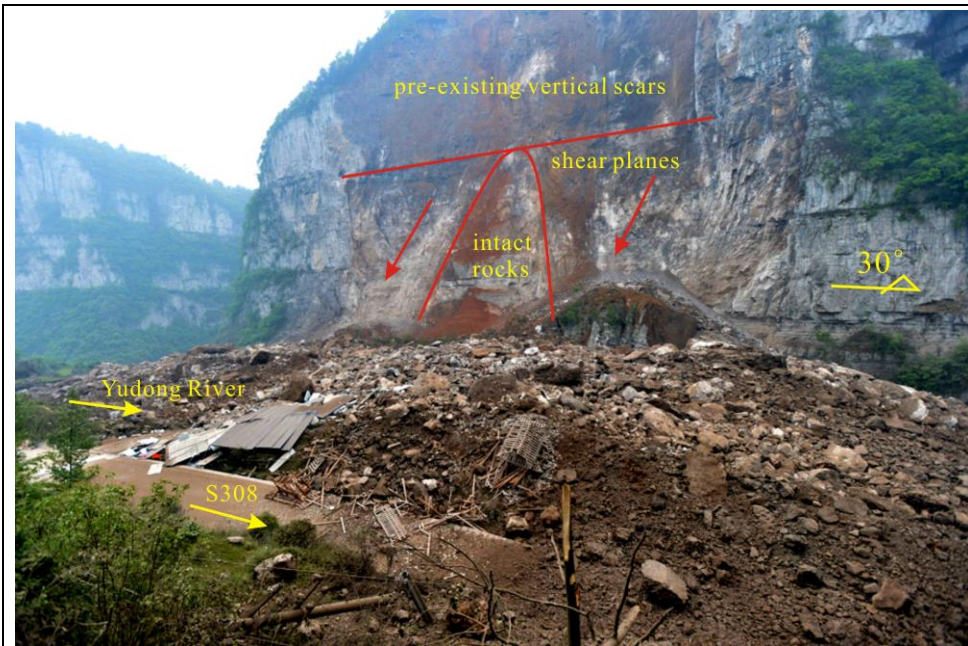


Fig. 6 Photograph showing rock slide II at Yudong. The pre-existing vertical scars are coated with karst of a yellowish-brown color, while the rupture surfaces are white and gray, indicating brittle failure and planar sliding through the limestone.

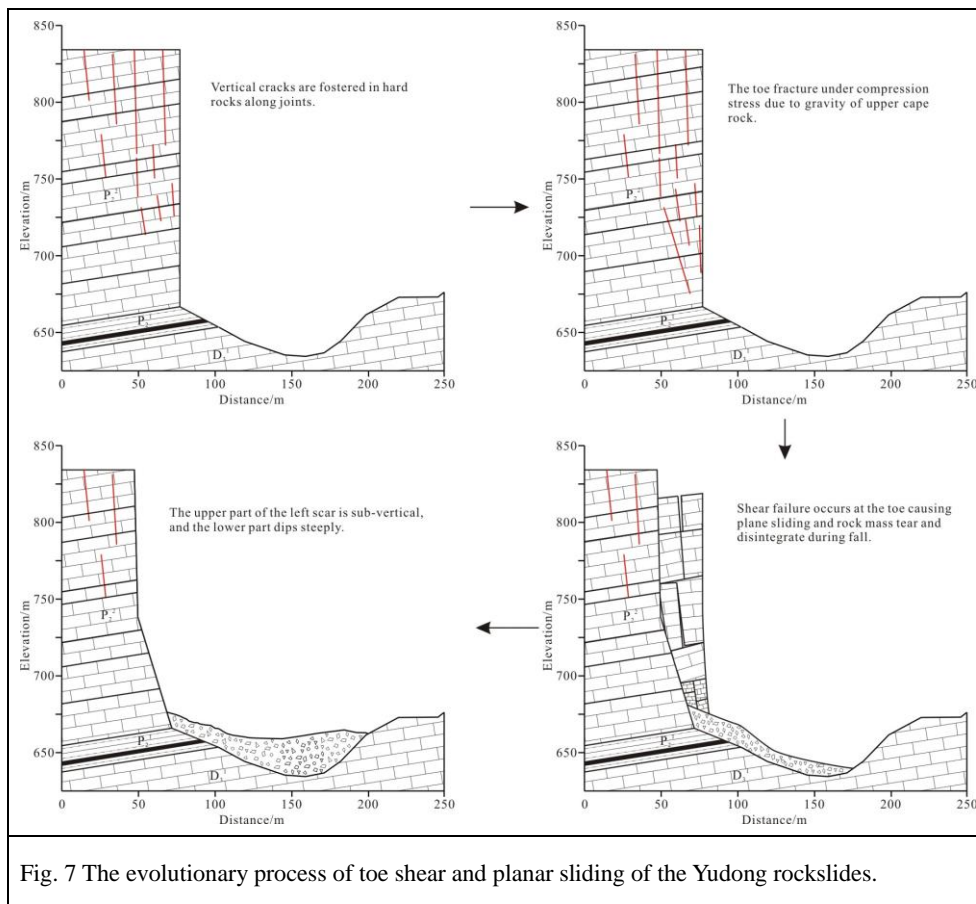


Fig. 7 The evolutionary process of toe shear and planar sliding of the Yudong rockslides.

158

### 159 3.2 Rock collapse at Zengzi Cliff

160 Zengzi Cliff lies in the gentle and wide core of the Jinfo Mountain Syncline, Nanchuan County  
 161 of Chongqing, in a “hard on soft” landform. The vertical limestone consists of two platforms  
 162 separated by softer rock (Fig. 8). Two major tectonic joints in the hard rocks strike at  $N40^{\circ}\text{--}50^{\circ}\text{E}$   
 163 and  $N30^{\circ}\text{--}50^{\circ}\text{W}$ , with dip angles of  $70^{\circ}\text{--}88^{\circ}$ . These two sets of joints are approximately  
 164 orthogonal to each other and perpendicular to bedding. The bedding trends at  $300^{\circ}\text{--}305^{\circ}$  with a  
 165 very low inclination ( $4^{\circ}\text{--}7^{\circ}$ ). The upper platform is U in shape; hence, the steep slope varies from  
 166 anaclinal to plagioclinal and cataclinal in different parts of the edge. Beneath the cliff,  $S_2$  silty  
 167 shale forms a soft base and a gentle slope ( $20^{\circ}\text{--}30^{\circ}$ ). Talus occurs everywhere under the cliffs,

168 indicating that cliff failure occurs as scarp retreat.

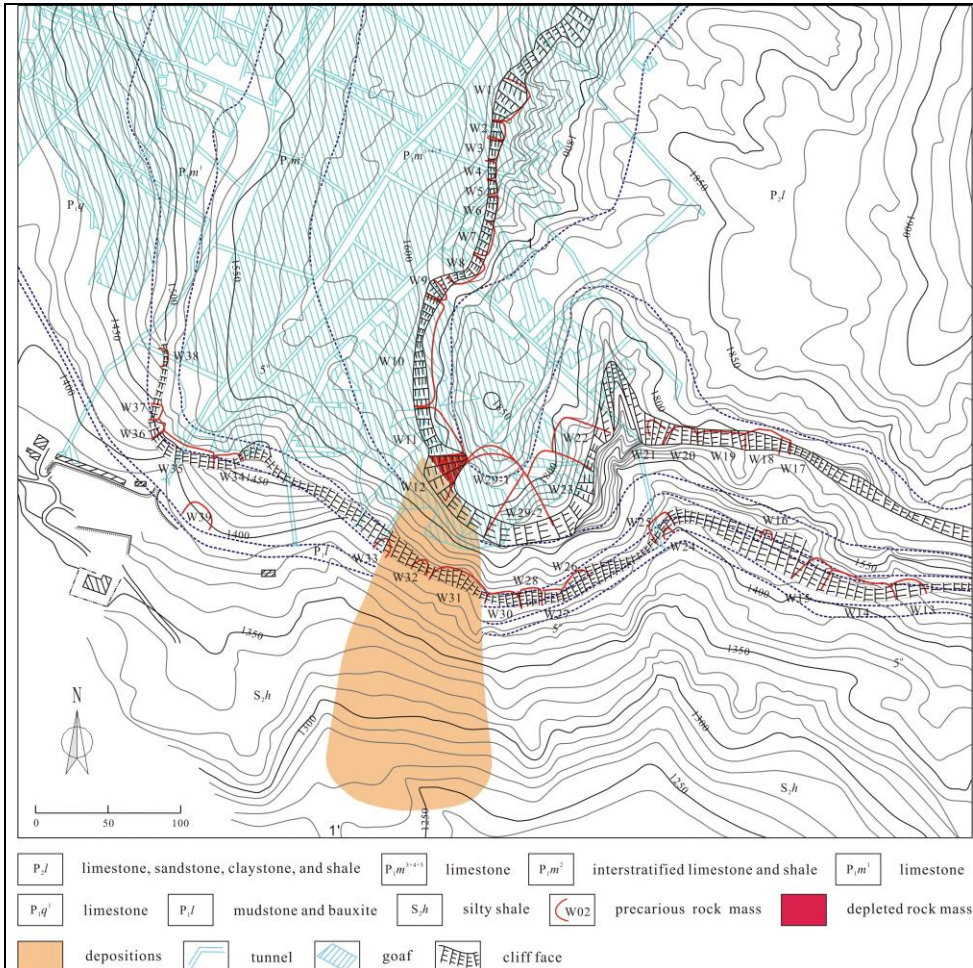


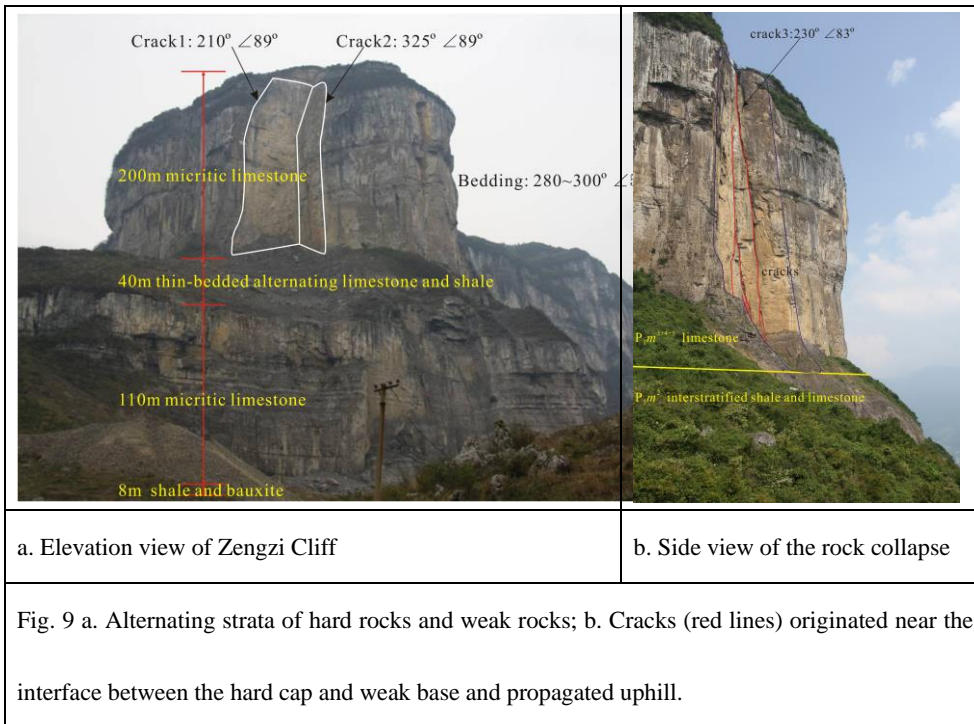
Fig. 8 Topographic map of the Zengzi Cliff area and the distribution of precarious rock masses on its edge. Room and pillar mining has been conducted in the P<sub>1</sub>l sequence since 1983, and the goaf extends from south to north. The depth of the goaf is about 100–120 m for the first step and 350–400 m for the second step.

批注 [I13]: Q: the depositions shadow is seem to somewhere strange, because the slope direction is SWW, but the shadow direction is just S, so i think the shadow range need to modify.  
A: The depositions is in the right place and it did turn to the south when it fell down to the slope surface.

169

170 Rocks frequently fall in the Zengzi Cliff area. On August 12, 2004, a massive rock collapse  
171 occurred in the upper platform, which is about 200 m high (Fig. 9). The depleted mass is a prism  
172 block shaped by sub-vertical joints and bedding. Two vertical back scars and a groove surface in

173 the underlain soft strata are exposed after the collapse. Large areas of the scars are coated with  
 174 karst argillaceous fillings and yellowish-orange calcite, while the rock bridge failure scars are  
 175 fresh. Field investigations showed that the head scars are wide open prior to the massive collapse.  
 176 Seepage forces and frost from percolating water acted on the prism block over a long time and  
 177 influenced the stability; however, only karst could alter the conditions in the rock adjoining the  
 178 slope by increasing the connectivity of back scars. The underlying soft strata consist of alternating  
 179 beds of thin-bedded shale and medium-bedded limestone, and as a result of weathering, form a  
 180 40-m-high slope.



181

182 Mining activity has been conducted for decades, but community monitoring started in 2001.  
 183 The opening velocity of the head scar was very slow from 2001 to 2003 (Ren, 2005). It increased  
 184 to 4–15 mm/10 d in the period between April and July 2004 (Fig. 10), and signs of pre-collapse,

185 (rock falls) were repeatedly observed. At that time, the government issued warnings and evacuated  
186 residents and workers. The velocity abruptly increased from August 10, and the increment reached  
187 658 mm on the last day. The process of the Zengzi rock collapse was captured on video: the tower  
188 dropped vertically and disintegrated while falling. It is unusual that the failure initiated in the  
189 bottom of the hard block rather than the underlying soft strata. The splitting of the hard rock mass  
190 at the toe led to tower collapse. The curved surface in the soft strata will have been carved by  
191 collision.

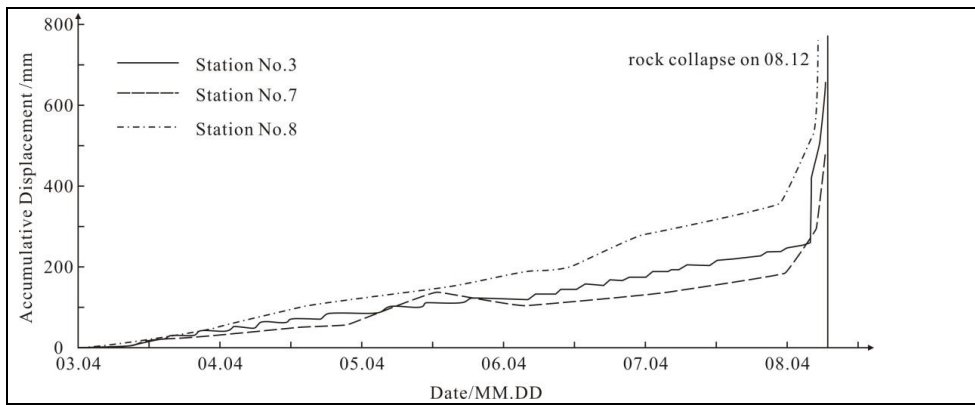


Fig. 10 Cumulative displacement of monitoring stations at the crest of Zengzi Cliff in 2004 (Ren, 2005).

192

193 Tensile splitting has been observed in uniaxial compression tests of rock samples with high  
194 brittleness and strength, such as limestone. There are several reasons why the collapse did not start  
195 with shear failure in the underlying strata. The rock mass in the bottom of the tower block is in  
196 poor condition: fractured and weathered. Drill cores obtained strongly karstic rock containing  
197 dissolution pores, caves, tufa, and calcite. The drilling also revealed at least 11 fissures, some of  
198 which were filled with yellow clay (107 Geology Team, 1995). This is because the underlying  
199 strata are low-permeability soft rocks; hence, there are steady water flows immediately above.

200 Furthermore, the soft strata are not sufficiently weak. These strata consist of interbedded thin  
 201 layers of shale (0.1–0.2 m) and medium-thick limestone. The tower block could easily shear  
 202 through the shale but not the intercalated limestone. Under these circumstances, tensile split  
 203 failure of the tower bottom is a reasonable failure mechanism, involving compression fracturing  
 204 and horizontal shearing in the shale beds (Fig. 11). Field studies and deformability tests on rock  
 205 masses all around the world have demonstrated that folded and flat-lying rock masses are prone to  
 206 tensile splitting near thin weak planes. Compression fracturing and tensile splitting are important  
 207 failure mechanisms for sub-horizontally bedded slopes. The Zengzi cliff collapse exposed back  
 208 scars in the nearby deformable rock mass, which propagated uphill (Fig. 9b), and a fractured rock  
 209 mass was observed near the shale interface.

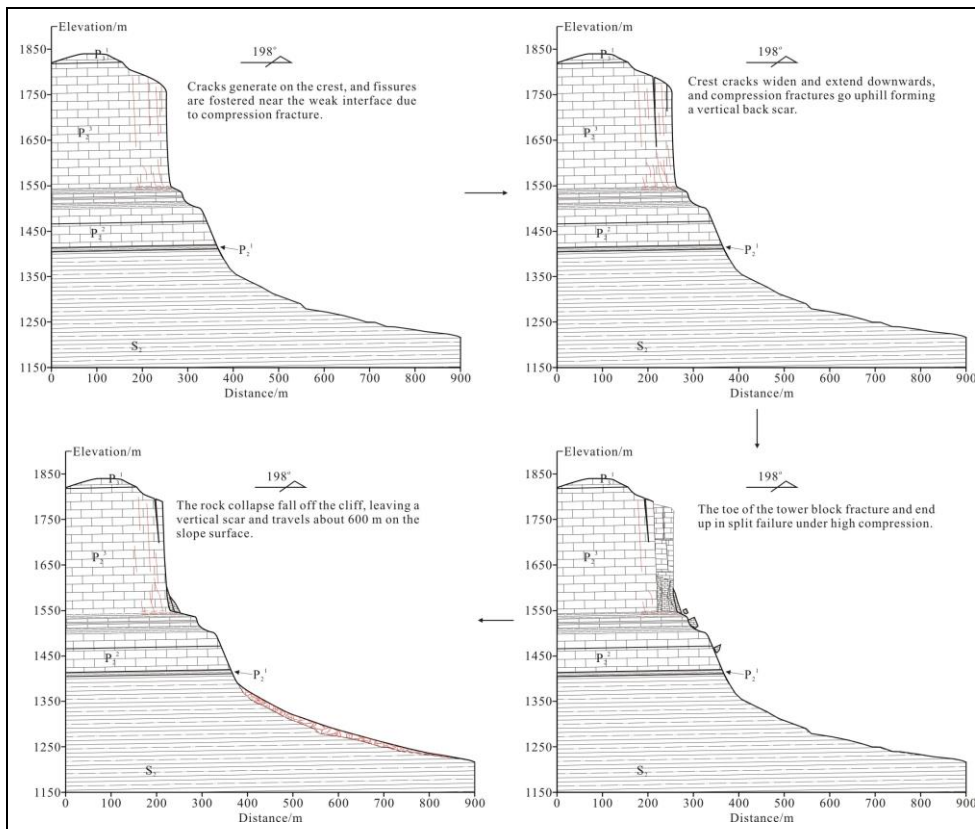


Fig. 11 Failure process of the Zengzi rock collapse, involving toe splitting and tensile failure.

210

### 211 3.3 Rock slump at Wangxia Cliff

212 When the base is sufficiently weak, and there is a steep fracture separating the column from the  
213 slope in the cap area, a rock slump with back-tilting mechanism is likely to occur. The Wangxia  
214 Cliff failure slump mechanism involved isolated limestone block breaking through shale at the toe,  
215 with rotational movement. The Wangxia Cliff is situated at the top of the left bank of the Yangtze  
216 River in Wushan County of Chongqing, about 1000 m above the water level (Fig. 12). Located in  
217 the flat core of the Hengshixi Fold, the bedding is slightly inclined ( $3^{\circ}$ – $8^{\circ}$ ) and strikes at  
218  $335^{\circ}$ – $340^{\circ}$ , opposite to the cliff face. Interbedded shales, mudstones, and coal seams form a gentle  
219 slope and separate the  $P_3$  limestone into two cliff steps. A country road passes over the slope  
220 below the 70–75-m high limestone escarpment, which contains several isolated slab- and  
221 prism-shaped blocks. On October 21, 2010, a prism with a volume of  $7 \times 10^4 \text{ m}^3$  became a rock  
222 slump failure.

批注 [I14]: Q: left or north

A: It is revised into “left”

批注 [I15]: Q: The geological age  
should be marked consistently only  
using symbols or texts.

A: The texts are replaced by symbols

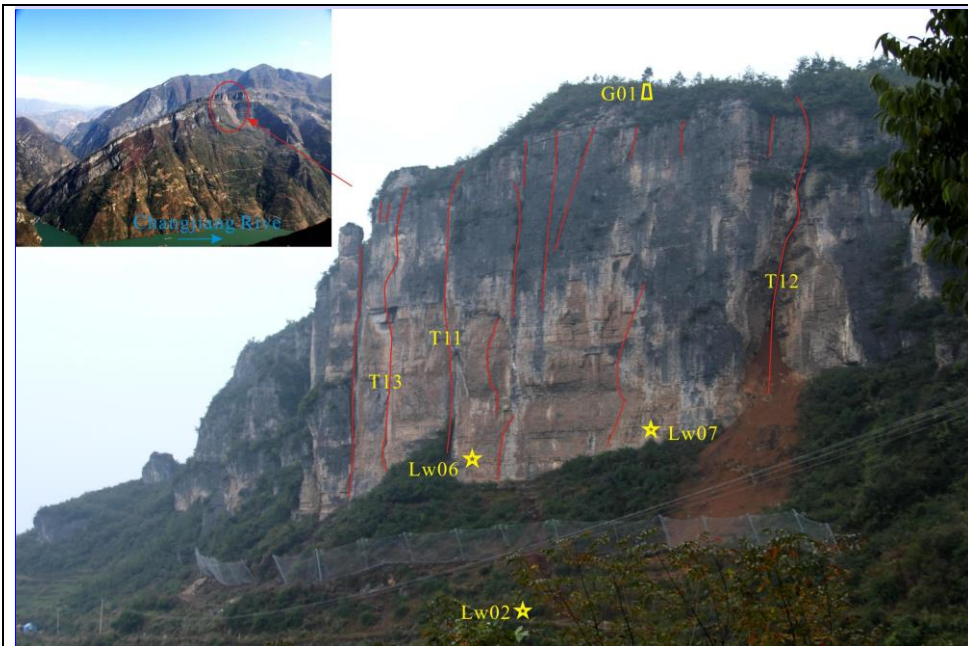


Fig. 12 Overview of Wangxia Cliff prior to the catastrophic rock slump. G01 represents a GPS station, and Lw02–Lw07 indicate the displacement monitoring stations. The rock slump of October 21, 2010 was controlled by vertical scars T11 and T12. The red lines represent fissures in the rock mass.

批注 [S16]: Q: the flow direction is wrong.  
A: The flow direction of the Changjiang River is revised (in the top left corner).

223

224 The slope movement can be traced back to June 18, 1999. Four collapsecraters and nine cracks

225 were observed in the crest area after 108.5 mm of rainfall on June 15 and 16 (Le, et al., 2011).

226 Intensive deformation began on August 21, 2010, after four days of concentrated rainfall. Rep

227 eated pre-collapse signs were observed. Crown cracks widened, and new cracks occurred on the

228 crest. Rocks fell off from the cliff face and vertical scars in the rock mass. In addition, gravelly

229 soils flowed out from steep cracks at the toe. Transverse ridges and cracks were observed on the

230 country road beneath. The mass movement accelerated as a result of 70 mm of precipitation from

231 October 10 to 13. The fissures in the isolated blocks extended and widened. Rock falls became

232 more obvious both in volume and frequency. Finally, a massive rock slump occurred on October  
233 21, in which the isolated prism slid downhill, breaking through the toe and leaning against the  
234 back scars. The underlying weak rocks were squeezed out and scattered over the slope surface.  
235 Displacement monitoring showed that the crest was dominated by subsidence, while the horizontal  
236 and vertical displacements were about the same at the base. The incompetent base showed  
237 horizontal movement and little subsidence (Fig.13). These phenomena were caused by ductile  
238 yielding and rotational shearing in the incompetent base (Fig. 14). The squeezing out contributed  
239 to the uphill propagation of cracks and disintegration of the mountain into slab- and prism-like  
240 blocks.

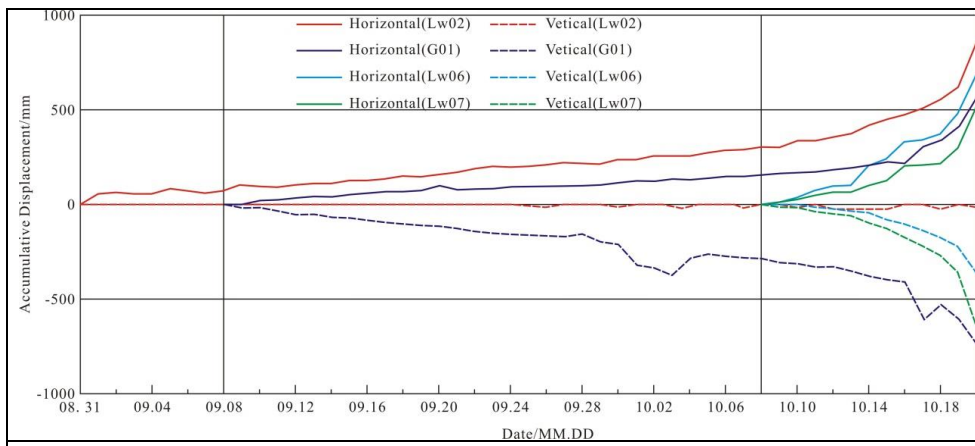


Fig. 13 Cumulative displacement at monitoring stations at the Wangxia rock slump (Le, et al., 2011).

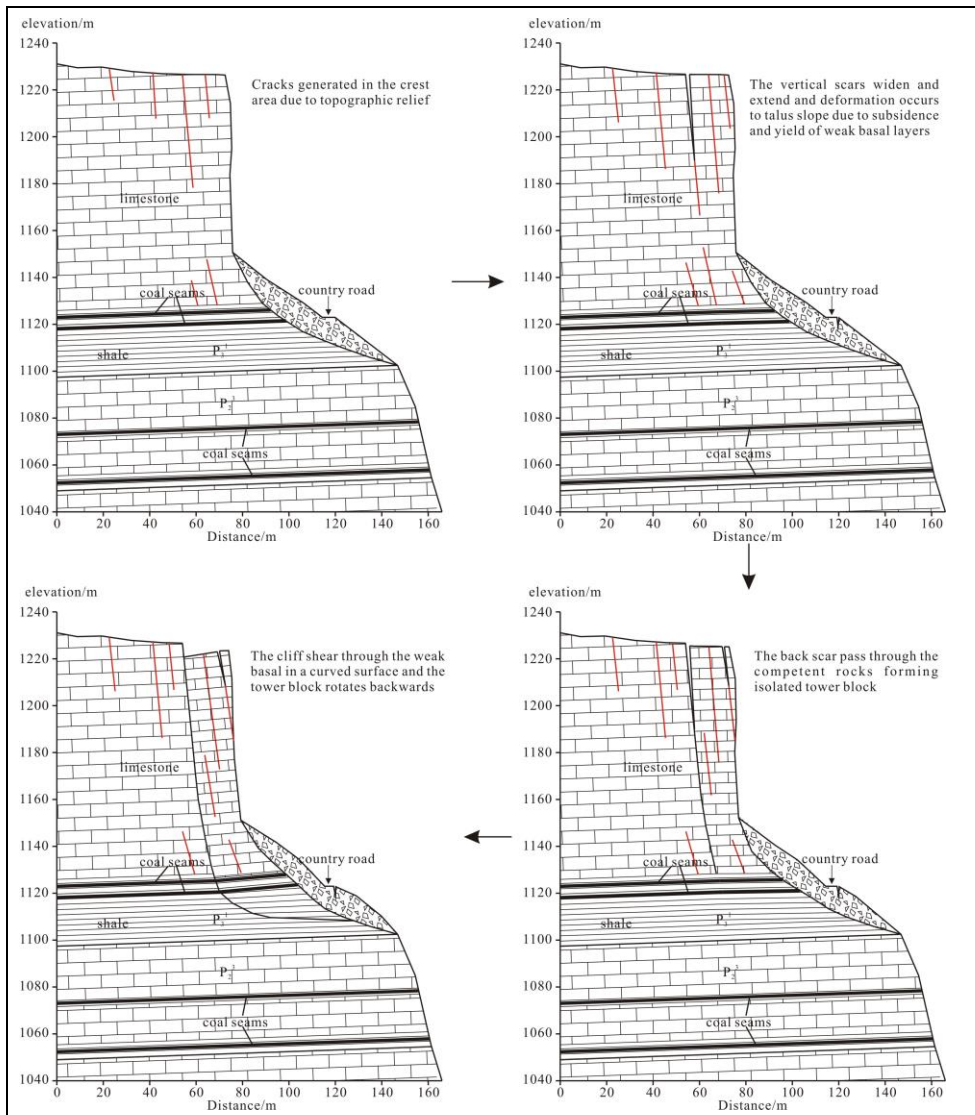


Fig. 14 Deformation and failure processes of the Wangxia rock slump.

241

242 It is worth mentioning that there is a good correlation between the acceleration of displacement  
 243 and concentrated rainfall. Because of cracks and fissures in the limestone, water could easily and  
 244 rapidly percolate into the weak strata. The unconfined compressive strength (UCS) of the shale  
 245 shows a substantial decrease when saturated, and the softening factor is about 0.62. However,  
 246 there is a 2-4 day time lag between concentrated rainfall and acceleration of displacement,

247 because the infiltration of water into poorly permeable shale takes time.

248

#### 249 4. Numerical back-analysis

250 Numerical analysis is a sophisticated method for assessing the potential failure modes of rock

251 slopes. We use it herein to validate the cases discussed above, which show different failure

252 mechanisms for sub-horizontally bedded cliffs (compound slide, rock collapse, and rock slump)

253 and to explain the backgrounds to the slides. The computation was performed using the computer

254 program UDEC. As discussed, the Yudong rock slide and Wangxia rock slump are characterized

255 by thick shale underlying the cap rock. However, the base of the Zengziyan consists of limestone

256 interbedded with thin shale bands. The calcareous shale in Yudong slide possesses a relatively

257 high strength and the thin shale bands, containing talcum, in Zengziyan collapse is easily

258 weathered and weak. The strength of the carbonaceous shale in Wangxia is moderate comparing to

259 the others. The parameters used in the simulation are given in Table 1.

260 Table 1 Parameters used in the numerical simulation

parameter	limestone	shale		
		Rock slide	Rock collapse	Rock slump
Thickness (m)	170	20	2	20
Density(kg/m <sup>3</sup> )	2700	2640		
Young's modulus, E(GPa)	65	5		
Poisson'sratio	0.13	0.2		
Friction angle of rock mass (°)	32	28	20	25
Cohesion of rock mass (MPa)	1.3	0.8	0.4	0.5

**批注 [I17]:** Q: If you do not discuss or figure out the difference of the three example, the numerical model will be seen to sudden, and it is not easy to understand why the three are different.  
A: A short discussion is presented from line 254-259 to explain the difference of the weak strata between these cases.

Tensile strength of rock mass (MPa)	0.3	0.1	0.04	0.04
Friction angle of joints (°)	30	25		
Cohesion of joints (MPa)	1.0	1		
FOS	-	1.01	1.21	1.07

261

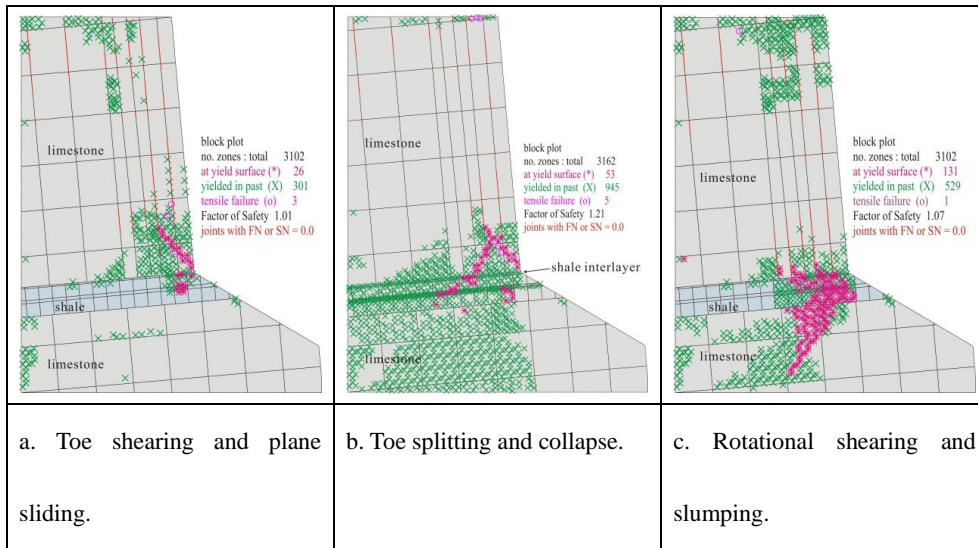


Fig. 15 Plastic state and joint opening for rockslide initiation in cliff slopes.

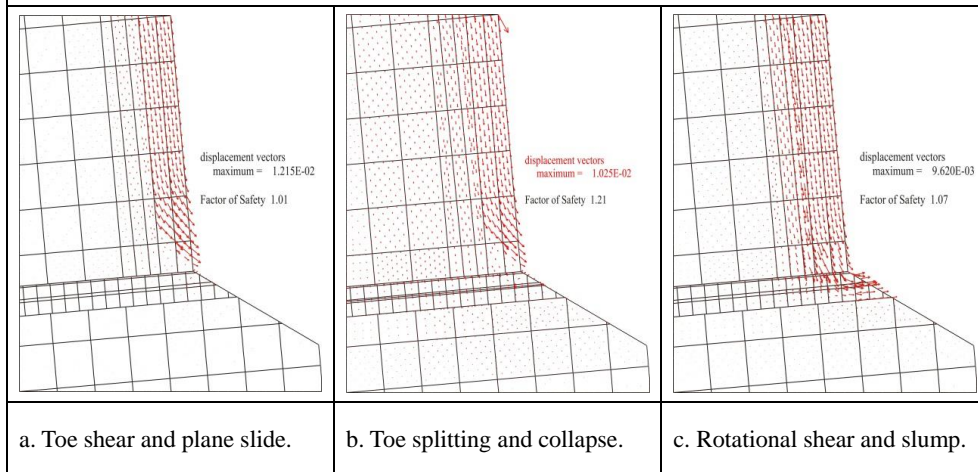


Fig. 16 Displacement vectors of the initial failures of cliff slopes.

262

263 The natural stress field is characterized by a tensile zone on the crest and stress concentration at  
264 the toe. When a thick incompetent basal layers is present, the jointed slope tends to fail as a slump.  
265 A yielding curved surface gradually emerges in the basal layers under long-term gravitational  
266 compression of the upper cap rock. A large plastic zone is present in the weak basal layers and  
267 nearby hard rock mass (Fig. 15c). The horizontal movement of the weak stratum is prominent.  
268 Pre-existing joints in the hard rock mass widen upward and slip with the ductile flow of the basal  
269 layers. The movement of the massive unstable rock mass is dominated by subsidence in the crest  
270 area and back tilting at the toe (Fig. 16c).

271 When the weak basal is a thin interlayer, rotational slide through the toe is unlikely to occur. The  
272 horizontal shear stress determines the possibility of shear failure in the beds. For a sub-horizontal  
273 bedded slope with gentle tectonic disturbance during geologic evolution, the horizontal to vertical  
274 stress ratio is generally less than 1 (Zhang, et al., 1994). This indicates that it is possible for a  
275 weak interlayer with a frictional angle less than  $45^\circ$  to shear horizontally. Under these  
276 circumstances, the plastic zone ranges over the interlayer as well as the overlying competent rocks.  
277 The rock mass at the toe is in a plastic state as a result of compression fractures. Two yield  
278 surfaces dipping in opposite directions are formed (Fig. 15b), similar to tensile failure behavior for  
279 some brittle rock samples. The displacement prior to collapse is limited, and remarkable squeezing  
280 out is unlikely to be observed in the toe area (Fig. 16b).

281 A rock slide might burst out in hard rock where back scars cut through, and no discontinuities or  
282 weak strata are exposed at the toe. Irregular scars caused by brittle and shear failure through rock  
283 mass dip out of the cliff faces. The yield zone is mainly located at the block toe but not in the  
284 underlying rocks (Fig. 15a). The fracture of the toe rock mass gives rise to joints opening

285 immediately above. Numerical computation gives a plane yield surface at the bottom of the  
286 separated block, which is called a potential failure surface (Fig. 16a). A small displacement  
287 appears before the outbreak of a compound slide. However, ground fractures on the crest and  
288 spalling in the toe area might occur.

289

## 290 5. **Underground mining**

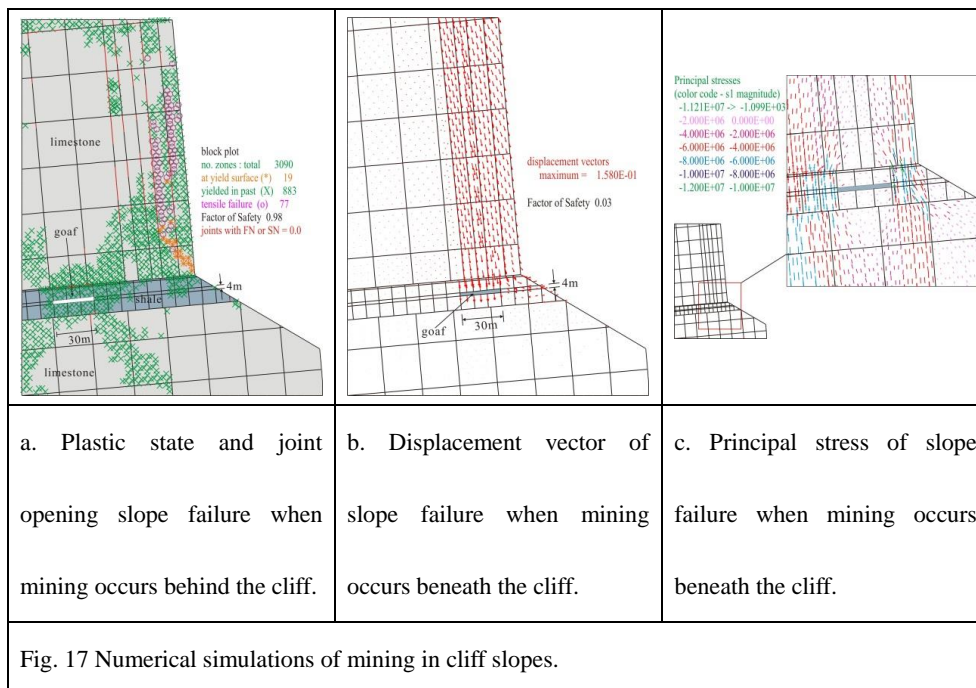
291 The failures at the three locations described above are related to large areas of mining out. Pells  
292 (2008) used a 2-D continuum model to assess macro-scale movements of cliff faces caused by  
293 total extraction and proved that the steep slope tends to tilt outwards when mining occurs beneath  
294 the cliff, and extraction well behind the cliff face causes back tilt. Our similar simulations are  
295 shown in Fig. 16. The rock slide model in Fig. 14a was adopted. The roof tends to collapse, and  
296 the surrounding rocks gradually fracture. The undermining-induced subsidence of the crest causes  
297 the dilation and tensile failure of the rock mass (Fig. 17a). The FOS decreases from 1.01 to 0.98  
298 when the underground mining is located behind the cliff face. When the extraction is directly  
299 beneath the cliff, the rock mass is subjected to a small constraint; hence, cliff failure break-out  
300 through the fractured rock mass between the goaf and open face is feasible (Fig. 17b). The  
301 maximum principal stress on both sides of the goaf increases while that of the overlying rocks  
302 decreases (Fig. 17c).

**批注 [I18]:** Q: I believe the under mining simulation is more like the Case 1 (Yudong Slide), what do you think how under mining affects the other two cases?

A: These three cases has a similar "hard on soft" landform and structure. The only difference is the rock mass at the toe which has been taken into account in the simulation. So that the simulation is adequate to assess under mining effects in these cases.

**批注 [I19]:** Q: I assume you mean a 2D continua model?

A: Yes. The "continuum 2-D model" is replaced by "2-D continuum model".



303

## 304 6. Conclusions

305 In this study, three different examples of failure in sub-horizontally bedded limestone cliffs are  
 306 discussed. The failures are characterized by pre-existed vertical joints passing through thick  
 307 limestone. The Yudong rock slide originated in a limestone cliff edge and left a moderately  
 308 inclined rupture plane, implying shear failure through the hard rock. Rock collapse caused by  
 309 compression fracture and tensile splitting of the rock mass near the interface between the hard cap  
 310 and weak stratum occurred at Zengzi Cliff. The Wangxia cliff failure showed a slow rock slump  
 311 sheared through the underlying incompetent rock mass along a curved surface. The mechanism of  
 312 toe breaking mainly depends on the strength characteristics of the rock mass.

313 Considering that the rock mass near the cliff face is not laterally constrained, it is reasonable to  
 314 assume that there is a massive UCS failure at the toe of the vertical tower and slab blocks.

315 Some failure characteristics of jointed rock mass in in situ UCS tests have been observed all

316 around the world, for both shear and tensile failure. Of special concern is tensile failure in  
317 horizontally bedded rock masses with interlayers. Compression fractures emerge near the  
318 interfaces and form vertical slabs, which eventually split. Another possibility is squeezing out of  
319 weak interlayers as a result of compression fracture, causing the hard rock nearby to yield to  
320 tensile stress and disintegrate. It is worth noting that the UCS of the rock mass in compression  
321 fracturing is much lower than that of intact rock. A criterion based on horizontal shear failure  
322 along weak interlayers and the UCS ratio of the cap and underlying rock masses could be used to  
323 assess the failure mode of tower and slab blocks on cliff edges.

324

### 325 **Acknowledgments**

326 This work was carried out with financial support from the China Geological Survey (No.  
327 12120114079101), the Ministry of Science and Technology of the People's Republic of China (No.  
328 2012BAK10B01) and the National Natural Science Foundation of China (No. 41302246).

329

### 330 **References**

331 107 Geology Team of Sichuan Geology and Mineral Bureau. (1995). Geology Survey Report  
332 on Bauxite Deposit of Loujiashan in Nanchuan, Sichuan (in Chinese).

333 Abele, G. (1994). Large rockslides: their causes and movement on internal sliding planes.  
334 Mountain Research and Development, 14(4): 315-320.

335 Altun A.O., Yilmaz I., Yildirim M. (2010). A short review on the surficial impacts of  
336 underground mining. Sci Res Essays, 5(21), 3206-3212.

337 Ding W.W., Yu Y.Z., Deng W.L., et al. (1990). Stability analysis of reservoir bank in Three

338 Gorges of Yangtze River. Center of hydrological and engineering geology, Ministry of Geology  
339 and Mineral Resource, Chengdu: 7-8. (in Chinese)

340 Embleton-Hamann C. (2007). Geomorphological hazards in Austria. *Geomorphology for the*  
341 *Future*, Innsbruck University Press, Innsbruck, 33-56.

342 Hungr O., Evans S.G. (2004). The occurrence and classification of massive rock slope failure.  
343 *Felsbau*, 22(2), 16-23.

344 Huang R.Q. (2013). Mechanisms of large-scale landslides and pre-recognition. Key note on  
345 the Six National Academic Conference of Geological Hazard. April 11-12, 2013. Beijing, China.

346 Kay D., Barbato J., Brassington G., et al. (2006). Impacts of Longwall Mining to Rivers and  
347 Cliffs in the Southern Coalfield. In Aziz N. (ed), *Coal 2006: Coal Operators' Conference*,  
348 University of Wollongong & the Australasian Institute of Mining and Metallurgy, 2006, 327-336.

349 Le Q.L., Wang H.D., Xue X.Q., et al. (2011). Deformation monitoring and failure mechanism  
350 of Wangxia Dangerous Rock Mass in Wushan County. *Journal of Engineering Geology*,  
351 19(6):823-830.

352 Li Y., Meng H., Dong Y., Hu S.E. (2004). Main types and characteristics of geo-hazards in  
353 China-based on the results of geo-hazard survey in 209 counties. *The Chinese Journal of*  
354 *Geological Hazards and Control*. 15(2):29-34.

355 Lollino P., Martimucci V., Parise M. 2013. Geological survey and numerical modeling of the  
356 potential failure mechanisms of underground caves. *Geosystem Engineering*, vol. 16 (1): 100-112

357 Marschalko M., Yilmaz I., Bednárík M., et al. (2012). Deformation of slopes as a cause of  
358 underground mining activities: three case studies from Ostrava–Karviná coal field (Czech  
359 Republic). *Environmental monitoring and assessment*, 184(11): 6709-6733.

360 Parise M. (2008) Rock failures in karst. In: Chen ZY, et al (eds) Landslides and Engineered  
361 Slopes. Proc. 10th Int. Symp. on Landslides, Xi'an (China), June 30–July 4, 2008, 1, pp 275-280

362 Parise M. (2010). Hazards in karst. In Proceedings International Interdisciplinary Scientific  
363 Conference “Sustainability of the Karst Environment. Dinaric Karst and Other Karst Regions.”:  
364 Series on Groundwater. IHP-UNESCO, Plitvice Lakes, Croatia (pp. 155-162).

365 Pells P.J.N. (2008). Assessing parameters for computations in rock mechanics. In Potvin Y,  
366 Carter J., Dyskin A., et al (eds), Proceedings First Southern Hemisphere International Rock  
367 Mechanics Symposium (SHIRMS), 1:39-54.

368 Palma B., Parise M., Reichenbach P., et al. 2012. Rock-fall hazard assessment along a road in  
369 the Sorrento Peninsula, Campania, southern Italy. *Natural Hazards*, 61 (1): 187-201.

370 Rainer P., Martin B., Rudolf H., et al. (2005). Geomechanics of hazardous landslides. *Journal*  
371 *of Mountain Science*, 2(3), 211-217.

372 Ren Y.R., Chen P., Zhang J., et al. (2005). Early-warning analysis on the rockfall for  
373 Zengziyan W12# dangerous rock mass in Nanchuan City of Chongqing. *The Chinese Journal of*  
374 *Geological Hazard and Control*, 16(2):28-31

375 Rohn J., Resch M., Schneider H., et al. (2004). Large-scale lateral spreading and related mass  
376 movements in the Northern Calcareous Alps. *Bulletin of Engineering Geology and the*  
377 *Environment*, 63(1), 71-75.

378 Ruff M., Rohn J. (2008). Susceptibility analysis for slides and rockfall: an example from the  
379 Northern Calcareous Alps (Vorarlberg, Austria). *Environmental geology*, 55(2), 441-452.

380 Santo A., Del Prete S., Di Crescenzo G., Rotella M. (2007). Karst processes and  
381 slope instability: some investigations in the carbonate Apennine of Campania (southern Italy).

382 In:Parise M, Gunn J (eds) Natural and Anthropogenic Hazards in Karst Areas:  
383 Recognition,Analysis and Mitigation. Geol. Soc. London, sp. publ. 279: 59–72

384 Tang F.Q. (2009). Research on mechanism of mountain landslide due to underground mining.  
385 Journal of Coal Science and Engineering (China), 15(4):351-354.

386 Von Poschinger, A. (2002). Large rockslides in the Alps: A commentary on the contribution  
387 of G. Abele (193 7-1994) and a review of some recent developments. In: Stephen G Evans, et  
388 al.(eds), Catastrophic Landslides: Effects, Occurrence, and Mechanisms,:237-255.

389 White E., White W. (1969). Processes of cavern breakdown. Bull. Natl. Speleol. Soc.  
390 31(4):83–96

391 Zhang C.S., Zhang Y.C., Hu J.J.,Gao Q.Z. (2000). Spatial and temporal distribution  
392 characteristics and forming conditions of Chinese geological disasters. Quaternary Science.  
393 20(6):559-566

394 Zhang Z.Y., Wang S.T., Wang L.S.(1994). Principle of Engineering Geology Analysis. China  
395 Geology Press, Beijing: 66